TUNNEL DETECTION BY HIGH RESOLUTION SEISMIC REFLECTION METHODS

by
Don W. Steeples
Richard D. Miller
Ralph W. Knapp

of the
Kansas Geological Survey
Lawrence, Kansas 66046

Final report of research completed for
the Army Corps of Engineers
Waterways Experiment Station
Vicksburg, Mississippi

January 1987
Open-file Report #87-34

According to Figure Captions, No figure #8

INTRODUCTION

The detection and delineation of underground cavities from the surface by geophysical means is a desirable goal. Our research in cavity detection has been with seismic-reflection methods. This paper shows the results of initial experiments designed to detect cavities beneath the earth's surface in areas where no surface disturbance has occurred.

Previous seismic research intended to detect cavities due to salt-solution mining (Cook, 1965), lava-flow tunnels (Watkins et al., 1967), and abandoned subsurface coal mines (Fisher, 1971; Hasbrouck and Padget, 1982) has met with limited success. Most researchers using seismic techniques for cavity detection cite three phenomena for evidence of a cavity: free oscillations or resonance of the cavity walls, anomalous amplitude attenuations, and delay of arrival times (Cook, 1965; Watkins et al., 1967; Fisher, 1971).

Discriminating a subsurface void from the undisturbed material around it, using seismic-reflection techniques, depends a great deal on the dominant frequency of the recorded data. Widess (1973) determined that the minimum resolvable bed is 1/4 the wavelength of the recorded energy. Since frequency is inversely related to wavelength, the higher the dominant frequency the thinner the resolvable beds. Ability to detect cavities is also limited by shortness of wavelengths of the seismic energy.

Increasing the dominant frequency and the signal-to-noise ratio has enhanced our ability to detect subsurface voids. We have improved our signal-to-noise ratio by careful attention to geophone plants, minimiz-

ing environmental noise, and controlling the air-coupled wave from the seismic source. Increasing the dominant frequency of the recorded data can be done by increasing the frequency of the low-cut filters of the recording system, proper selection of a seismic source, and careful attention to static correction and velocity analysis during the digital processing of the data. It must be kept in mind, however, that the amount of high-frequency information detected by the geophones is dependent to some degree on the geologic conditions in the near-surface.

CAVITY DETECTION IN GRANITE

Voids in hardrock are deceivingly difficult to detect with reflection seismology. Since the acoustic impedance contrast at a boundary is the major determining factor in the amount of seismic energy reflected, an air-filled cavity in rock results in almost total energy reflection. Recording clear unobscured reflection events from the top of cavities is not as clear-cut as theory might predict. A combination of inhomogeneties in the rock and the size of the cavity with respect to the dominant wavelength complicate the recorded data, making standard CDP-reflection acquisition and processing techniques ineffective.

In order to determine the seismic parameters that are critical to cavity detection in hardrock areas (i.e., granite, basalt, limestone, dolomite, etc.), we conducted experiments across the top of a known tunnel in solid granite. The site selected for field experiments was the Moffat railroad tunnel near Winter Park, Colorado. The railroad tunnel is 6 m (19 ft) in diameter, and we performed surface seismic-reflection surveys across the tunnel where it was 19 m (62 ft) and 80 m (262 ft) below the earth's surface.

The results of the seismic survey above a 19-m (62-ft) deep location are shown in Figure 1. The data presented are a 2-fold CDP stack of traces with source-to-receiver distances from 18.3 to 20.1 m (60 to 66 ft). The strong event at 40 to 50 msec between CDP 295 and CDP 325 represents direct detection of the top of the tunnel. The inverted bowl shape of this event is a result of the curvature of the tunnel ceiling in combination with the gradual progression of the shot and receivers down the line. The frequency of this reflecting event is about 180 Hz. Directly below this feature between 70 to 120 msec is a series of lower-frequency events pulled up similar to the event at 40 msec. The dominant frequency of these deeper events is about 100 Hz. We believe these to be a resonance phenomenon associated with the interaction of the seismic energy with the tunnel. The high-frequency events between 50 and 70 msec on the stacked section are the air-coupled wave from the rifle source.

In order to test our resolution capability for tunnel detection, we moved our experiments up the mountain to a surface location about 80 m (262 ft) above the tunnel. Stacking 5 shots from a downhole 50-cal resulted in the highest quality records, however, for field efficiency reasons the surface 50-cal was used to collect the CDP data. Average field files from both types of sources are shown on Figure 2. The inverted bowl-shaped feature, obvious on the downhole 50-cal data, was clearly identifiable on more than 50 of the surface 50-cal field files used in later processing. Preliminary filtering greatly enhanced the curved arrival on Figure 3. Figure 4 shows the raypath that would be involved in diffractions from the tunnel. Note that a geophone directly above the tunnel is always the first geophone to sense the diffracted

seismic waves from the tunnel. This means that moving the shotpoint away from the tunnel increases the arrival time of the diffracted waves at all geophones, but the specific geophone directly above the tunnel always has the earliest arrival of the diffraction. The diffraction model can explain the arrival pattern, but not the velocity derived from the shape of the parabola on the field files in Figure 2. The observation of a diffraction-type event on multiple field records is encouraging but not conclusive. Still unexplained is the abnormally low velocity calculated from the parabolic curve always symmetric about receiver 350.

Parallel to the railroad tunnel discussed above is the Moffat water tunnel. The water tunnel is about 2.5 m (8 ft) in diameter and is about 17 m (55 ft) horizontally distant from the railroad tunnel. Our early experiments in the vicinity of the railroad tunnel did not reveal reflections or diffractions from the water tunnel. Since the railroad tunnel is air-filled and the water tunnel is water-filled, we considered whether the acoustical impedance contrast (reflection coefficient) was possibly small enough that the reflected and diffracted waves were of too low amplitude to be detected. The velocity of P-waves in water is almost exactly half that we observed for the granite (1,700 m/sec (5,568 ft/sec) for water; 3,354 m/sec, (11,000 ft/sec) for granite). Density of the granite is about 2.7 times the density of water giving a reflection coefficient of about 0.7 which is sufficiently high to give a good return of seismic energy.

Detecting the water tunnel was the next goal in the continued development and fine tuning of the reflection technique for imaging voids. We suspected the dominant frequency of the recorded energy was

not high enough to detect the smaller tunnel. Returning to the experimental site 19 m (62 ft) above the Moffat tunnel, we increased our low-cut filter frequency to 480 Hz from 340 Hz and increased the energy of our source in hopes of increasing the dominant frequency while maintaining sufficient amplitude to record energy returning from the water tunnel. Field files recorded 19 m (62 ft) above the water tunnel (Figure 5) with the modified parameters show a very similar curved arrival pattern to that observed on the field files recorded 80 m (262 ft) above the railroad tunnel. This curved pattern, as before, always arrives first at the geophone directly above the tunnel and moves deeper in time as the source moves further from the tunnel. Also as before, the curvature of the arrival is much too slow to be a diffraction (from a theoretical point of view) in this geologic environment. The moveout on the curve 19 m (62 ft) above the tunnel is the same as that observed 80 m (262 ft) above the tunnel. Direct detection of the railroad tunnel at this depth is still possible with these modified parameters, and now a curved event seems to be indicative of the 2.5-m (8-ft) water tunnel approximately 17 m (55 ft) to the south of the railroad tunnel.

DETECTING WATER-FILLED CAVITIES IN COAL

Early mining practices in many cases did not include a detailed map of mined-out areas. Knowledge of exact locations of these voids is necessary to ensure safety and structural soundness in new construction. Locating these mines in the past has been done with tight-grid pattern drilling. We conducted several seismic-reflection surveys in the Pittsburg, Kansas, and LaCygne, Kansas, areas attempting to detect the presence of water-filled mines. Research in Pittsburg was conducted

in heavily drilled areas where voids in the coal seam had been located; whereas, in LaCygne, research was done in an area without much drilling.

Pittsburg, Kansas, Research

Seismic data were collected to enhance energy returning from the coal seam at about 10 m (33 ft) depth. The seam at 10 m (33 ft) varied from ½ (1.6 ft) to 1-m (3.3 ft) thick. Receivers and shots were spaced at ½ -m (1.6-ft) intervals resulting in ¼ -m (0.8-ft) subsurface sampling intervals. This subsurface interval would give us 8-12 traces within the average-size horizontal coal shaft. Our recording system I/O DHR 2400 has 24 recording channels and was sampling each channel every ¼ msec for 125 msec. Each channel had a pre-A/D low-cut filter with 24 dB/octave rolloff from the -3dB point of 340 Hz. The receivers were undamped, single 100-Hz geophones. The energy source was a 30-06 rifle modified with a silencer that doubles as a blow-out containment device.

A 24-channel field file is displayed in Figure 6 along with a sketch of the geology and approximate raypaths for the nearest and furthest offset traces. Some of the geophones were located over intact coal and others were over a void. The area indicated on the right side of Figure 6 shows reflected waves recorded over the intact coal seam. The results of the uphole survey (small explosive charge detonated at the coal depth) confirmed this reflection to be from the coal seam. The area indicated on the left side of Figure 6 represents the signal received over the void. Reflections from the void are clearly different than those from the coal.

The stacked CDP seismic section is displayed in Figure 7 along with an interpreted geological cross section. Line 1 was shot across two

boreholes, one at CDP location 260 indicating a cavity at 9 m (29 ft) and one at CDP location 346 indicating intact coal at 9 m (29 ft). Surface collapse between CDP locations 350 and 405 is approximately 0.7 m (2.3 ft) deep and is also indicative of a cavity in the subsurface.

The event occurring at 23-25 msec throughout most of the section was confirmed by the uphole survey as a reflection from the top of the coal seam. Areas in which amplitude of this event diminishes are interpreted as cavity. These areas correlate well with where drillhole data and surface collapse indicate cavity in the subsurface. Loss of amplitude of this event over water-filled cavities is attributable to contrast of the reflection coefficients. The acoustic velocity of water in the cavities is greater than the acoustic velocity of the coal, and the overlying shales have an even higher velocity. The reflection coefficient for the boundary between the water and shale will therefore be smaller than the reflection coefficient for the boundary between the coal and shale, yielding a reduced reflection amplitude over the water-filled cavities.

Overall quality of data was good enough to define the voids' boundaries. The top and bottom of a 1-m (3-ft) thick coal seam at depths of 9 and 13 m (29 and 43 ft) were resolved. Reflected events from the top of the coal seam exhibited reduced amplitudes over water-filled cavities. Velocity pull-ups were observed in reflected events from the bottom of the coal seam beneath the water cavities. Lateral resolution of cavities was within an estimated 1-1.5 m (3-5 ft).

LaCygne, Kansas, Research

The partially-mined coal seam in the LaCygne area was approximately 9-12 m (30-40 ft) deep, varying in thickness from 0.6 to 1 m (2 to 3 ft). The optimum recording window was between 14.6 and 29.3 m (48 and 96 ft) offset from the source. Spacing the geophones at 0.6 m (2 ft) resulted in common midpoint gathers spaced at 0.3 m (1 ft) intervals. This allowed 8-12 stacked traces within an average-sized mined-out room. The recording equipment and analog filter settings were identical to those used for the Pittsburg experiments. As before, the seismic source was a modified 30-06 rifle and the receivers were single 100-Hz geophones (undamped).

The CDP brute stack displayed in Figure 9 shows several anomalous zones. It was determined by drilling that the only anomaly resulting from a void is located at CDP 540. Assuming that the anomaly at CDP 540 is indicative of all voids in the coal in this area, a processing flow to enhance the voids can be derived. Then data acquired, using the correct field parameters, can be processed in a production-type mode enhancing anomalous zones similar in character to the one at CDP 540.

DIFFRACTION ENHANCEMENT STACK

Theoretically, energy reradiated from a point source p at depth z will be detected first at receiver r_3 (Figure 10).

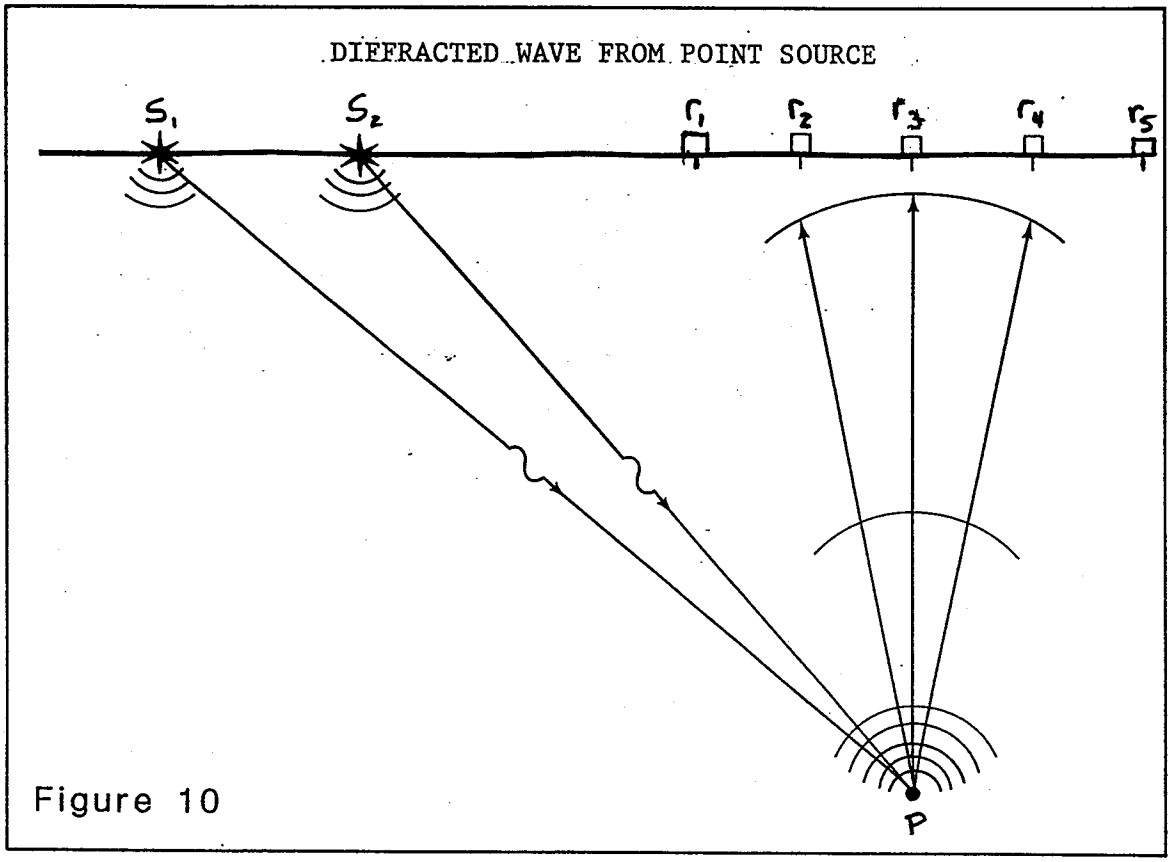

Figure 10

Recording and analyzing the energy reradiating from point source p requires no information about the original source of the energy. Therefore, all energy arriving at the receivers r not from the point source p can be cancelled or at least attenuated using an iterative stacking technique. Adapting the diffraction enhancement stacking technique to existing common depth point (CDP) software allows easy, yet effective use of the technique.

Seismic reflection data is commonly acquired to optimize future CDP processing. Most generally, in order to maximize redundancy and therefore increase the signal-to-noise ratio shotpoints and receiver stations have equal spacing and the source-to-receiver distances stay constant

throughout the profile. This allows data to be gathered into common midpoints, corrected for the moveout velocity of the reflections and stacked to enhance those reflectors.

As the source and receivers move down the profile in a consistant fashion, each subsurface point along the plane of the profile is sampled one-half times the number of recording channels and is separated from the previous subsurface point by one-half the source interval (which is also the receiver station interval).

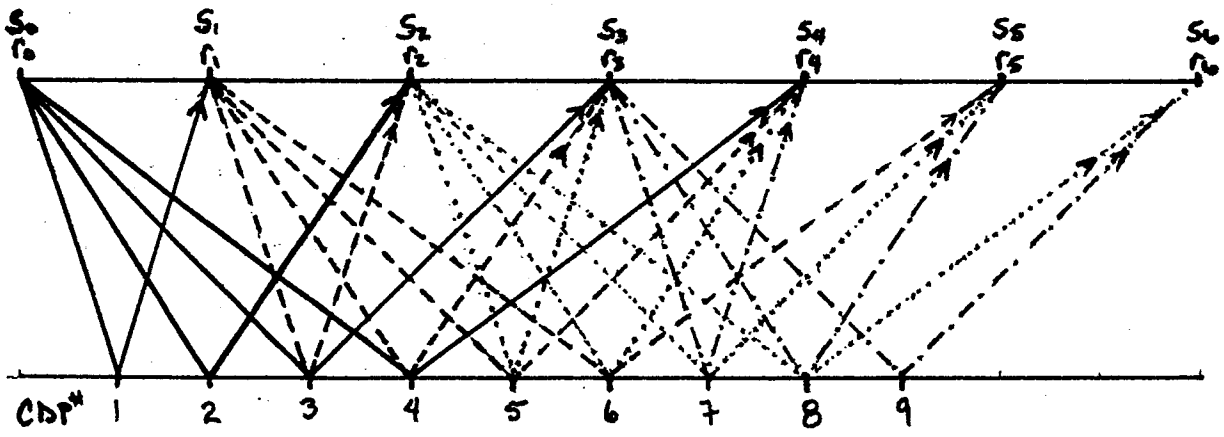

Figure 11

Shotpoint S_o, live receivers r_1, r_2, r_3, r_4

Shotpoint S_1, live receivers r_2, r_3, r_4, r_5

Shotpoint S_2, live receivers r_3, r_4, r_5, r_6

Shotpoint S_3, live receivers r_4, r_5, r_6, r_7

The same pattern is continued until the desired profile is complete. After the information has all been collected and is in field-file format, it can be sorted so each subsurface midpoint (which contains one-half times the number of recording channels) can be analyzed separately

and then stacked to enhance reflections. For the 4-channel case in Figure 11 all the shot-receiver pairs (S_o, r_2) that sample the subsurface point CDP #2 will be gathered together, each pair that samples subsurface point CDP #3 will be gathered together, and the same for CDP #4 and CDP #5, etc. The resulting data set will have traces collected in CDP gathers.

CDP #1	CDP #2	CDP #3	CDP #4	CDP #5
S_o, r_1	S_o, r_2	S_o, r_3	S_o, r_4	S_2, r_3
		S_1, r_2	S_1, r_3	S_1, r_4

CDP #6	CDP #7	CDP #8
S_1, r_5	S_1, r_6	S_2, r_6
S_2, r_4	S_3, r_4	S_3, r_5

Note: CDP data here is 2-fold.

The CDP method is very effective at attenuating linear-arriving events and enhancing reflected arrivals.

If, as in Figure 10, the apex of the diffraction is at receiver r_3 (indicating point source p is directly beneath r_3), then the power of the CDP method can be taken advantage of by assigning r_3 as the source location for every field file recorded regardless of actual field geometry. Then multifold seismic reflection data can be sorted and moveout focused on the shape and arrival times of the recorded diffraction wavefront.

The reflection raypaths are negated from the diagram and only the diffraction raypaths are shown in Figure 10. The arrival pattern of the diffraction curve from each shot at receivers r_1, r_2 curves from the

earliest arrival at r_2 to the latest at r_1. The same is true except mirrored for receivers r_4, r_5. Receiver r_4 would be earliest and r_5 would be latest. Receiver r_3 would always be the first receiver to detect the diffracted energy. This arrival pattern will be consistant with only the absolute time of the arrivals at the receivers changing as the real source and receivers rolled through.

The shape of the diffraction curve is theoretically dependent on the average velocity of the material above the point source. If the source is always assigned at S_3 ($S_3 = r_3$) and the live receivers roll through as the field notes indicate, then after correcting for terrain variations, the data can be gathered according to source offset. Each gather then contains only traces with a common-offset of receiver location r_3 (Figure 12). Next, by applying a NMO velocity correction to the sorted data, the diffraction will be flattened leaving all the arrivals except the diffraction distorted. Following the NMO correction, the data is stacked (Figure 13). The exact surface point over the tunnel can then be ascertained.

When the data quality is poor and no hint of a diffraction can be seen on the field data, this technique can be used in an interactive format. By setting up the geometry so the point source is assumed to be under r_1 and moving the receivers through as previously described for r_3, a moved-out stack results. Next, by repeating the process for r_2, and then r_3, and then r_4, etc. until all receivers are used, r_n stacked sections will result. Finally, stacking all r_n sections together according to assigned CDP numbers, the diffraction will enhance while all other arrivals are attenuated.

REFERENCES

Cook, J.C., 1965, Seismic mapping of underground cavities using reflection amplitudes: Geophysics, v. 30, no. 4, p. 527-538.

Fisher, W., 1971, Detection of abandoned underground coal mines by geophysical methods: USEPA Water Pollution Control Res. Ser., Proj. 14010, 94 p.

Hasbrouck, W.P., and Padget, N., 1982, Use of shear wave seismics in evaluation of strippable coal resources: Utah Geol. and Min. Survey Bull. 118, p. 203-210.

Watkins, J.S., Godson, R.H., and Watson, K., 1967, Seismic detection of near-surface cavities: U.S. Geol. Survey Prof. Paper no. 599-A, 12 p.

Widess, W.B., 1973, How thin is a thin bed?: Geophysics, v. 38, no. 6, p. 1176-1180.

FIGURE CAPTIONS

FIGURE 1. This 2-fold CDP stack of channels 8, 9, 10, and 11 has strong amplitude and frequency anomalies centered on CDP 310. The high-amplitude event at about 45 msec is interpreted as the top of the tunnel. The lower frequency oscillations below 80 msec could be resonance from the tunnel.

FIGURE 2. These field files were collected about 82 m (270 ft) above the railroad tunnel. The upper two field files are an average sample of the more than 50 files that showed the curved event. The lower 2 files are a 5-shot stack attempting to maximize the signal-to-noise. Note the returning diffraction-like event centered on receiver 350 (R350).

FIGURE 3. These field files are the same as in Figure 2, the only difference is a preliminary digital filter designed to enhance the curved arrival.

FIGURE 4. This schematic diagram shows the theoretical propagation from source to receivers when seismic energy encounters a point source.

FIGURE 5. The curved event present on the two field files is a result of the water tunnel. The source here was a downhole 30-06 rifle recorded with 480 Hz low-cut filters.

FIGURE 6. This field file was recorded with split-spread source/ receiver geometry. The source-to-closest receiver was 3.25 m (11 ft), and the farthest receiver was 8.75 m (29 ft).

FIGURE 7. This 12-fold CDP stacked section and interpreted geological cross section show voids in the coal seam. Four strong peaks between 10 and 30 msec dominate the seismic section. The shallowest doublet is a stacked refraction. Doublet directly below the refraction is a reflection from the coal. Amplitude drops in the coal reflector are interpreted as the top of the voids.

FIGURE 9. This 12-fold CDP stacked section has many anomalous zones. The anomaly that was shown by drilling to be indicative of water-filled voids in this ares is located beneath CDP 545.

FIGURE 10. This schematic diagram shows the theoretical propagation from source to receivers when seismic energy encounters a point source.

FIGURE 11. Raypaths of energy recorded by each live receiver for each shot during routine seismic reflection data acquisition.

FIGURE 12. This section has a strong diffraction-like event that has been enhanced. An example of the individual field files that were processed to obtain this section is displayed on the upper half of Figure 2. The estimated increase in signal-to-noise is 12 to 18 dB.

FIGURE 13. This section is a velocity corrected version of the section in Figure 12. The V_{nmo} used to flatten the curvature was 305 m/sec (1000 ft/sec).

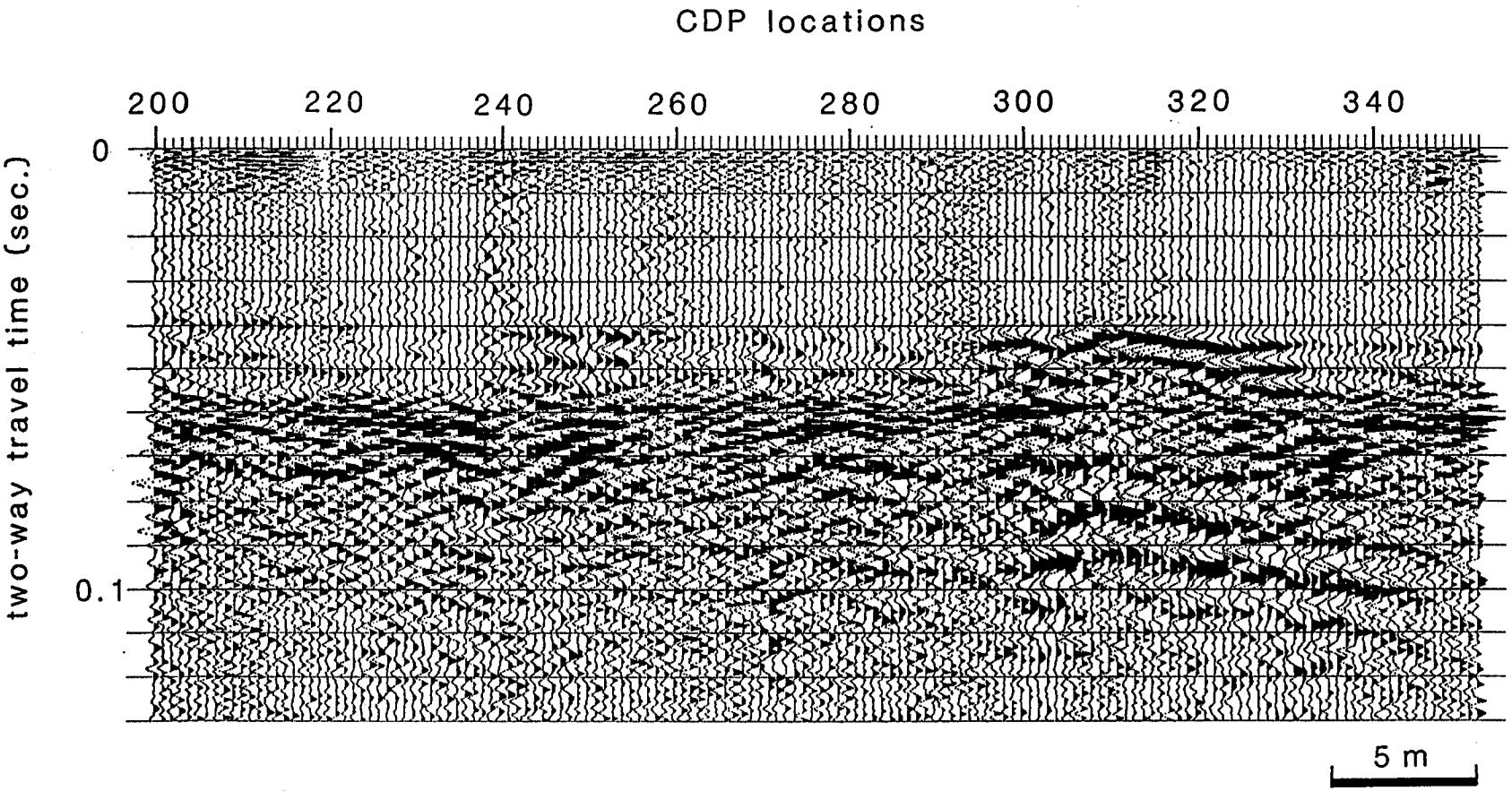
CDP locations
200
220
240
260
280
300
320
340
0
0.1
two-way travel time (sec.)
5 m

Figure 1

RAW FIELD DATA

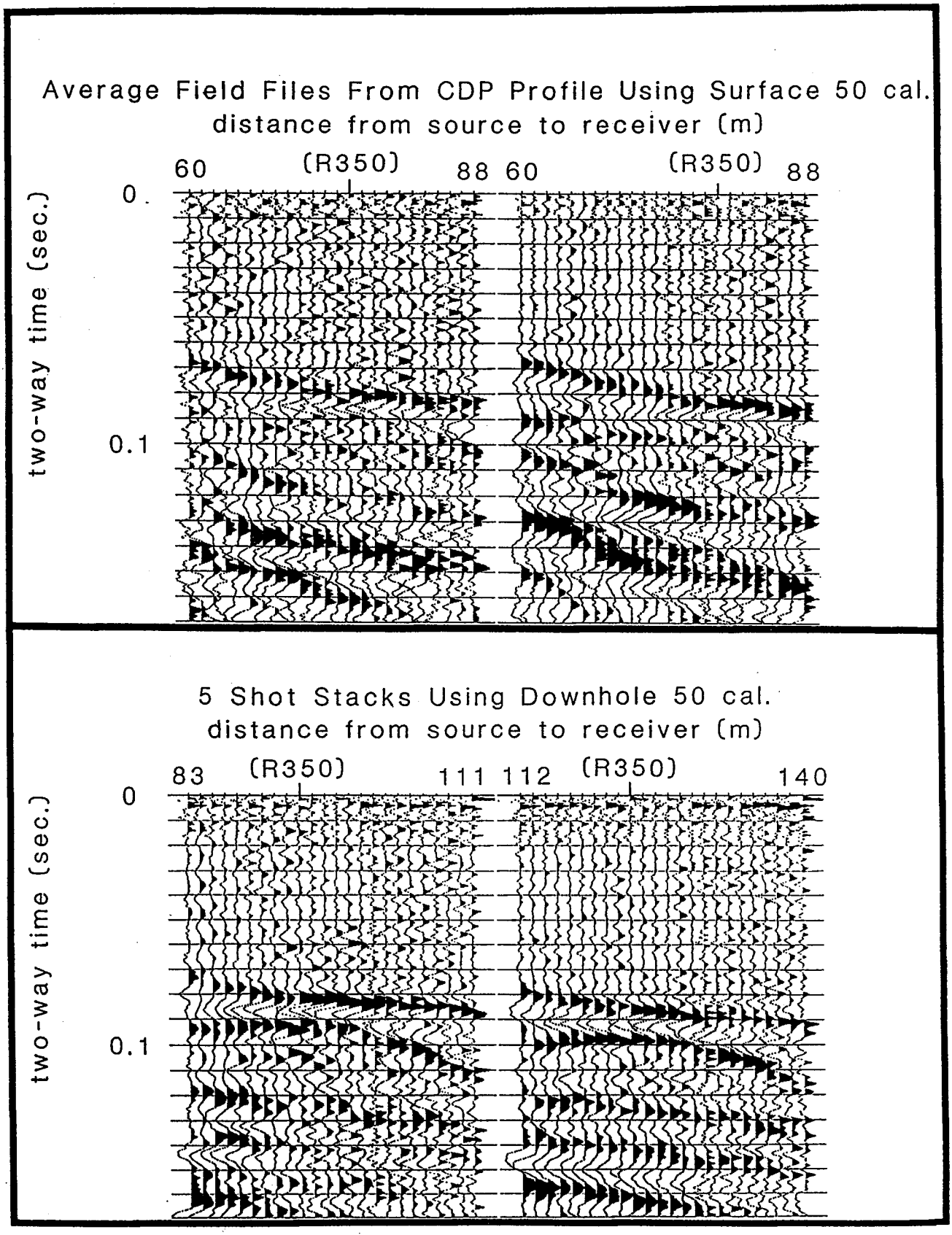

Figure 2

FILTERED TO ENHANCE DIFFRACTION

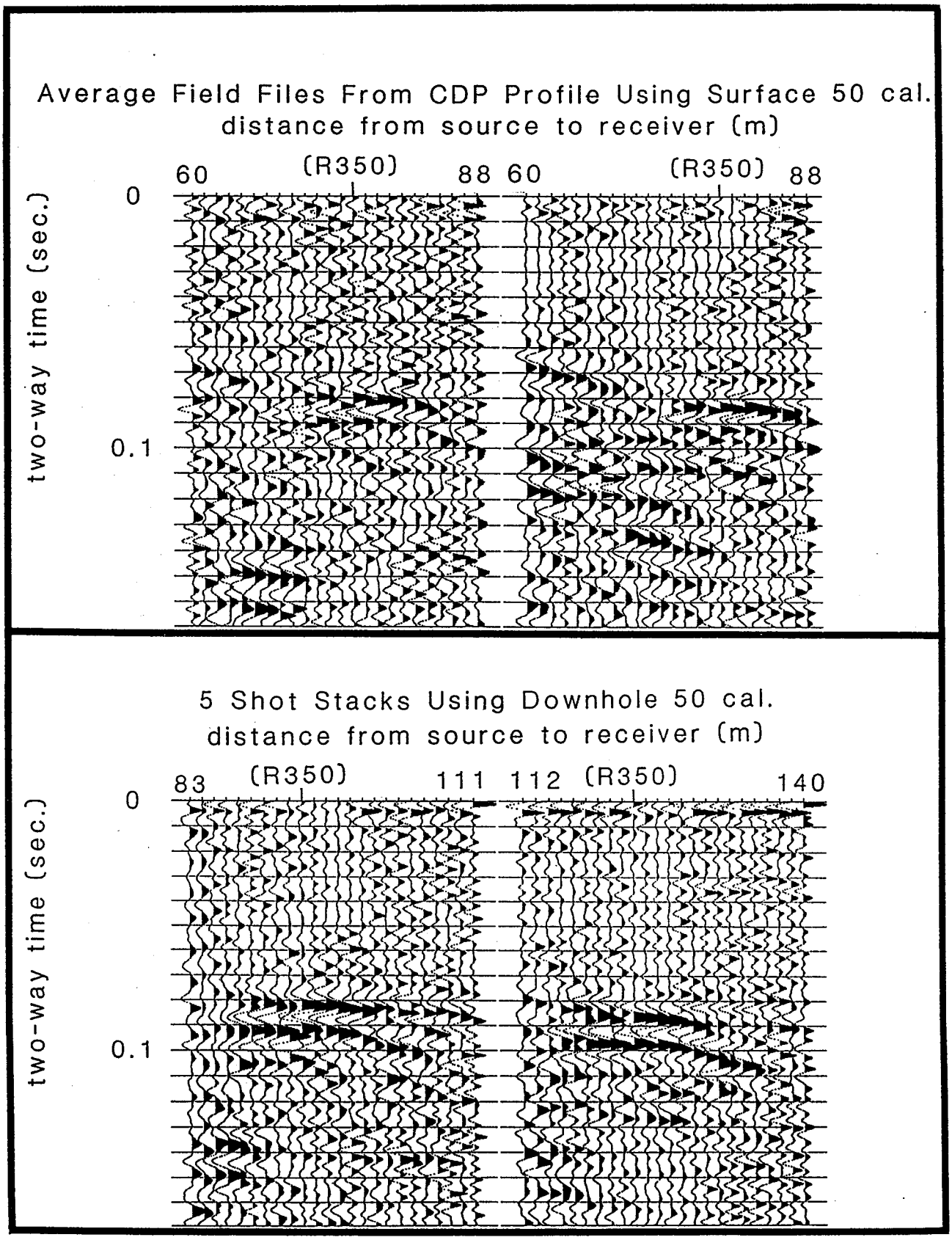

Figure 3

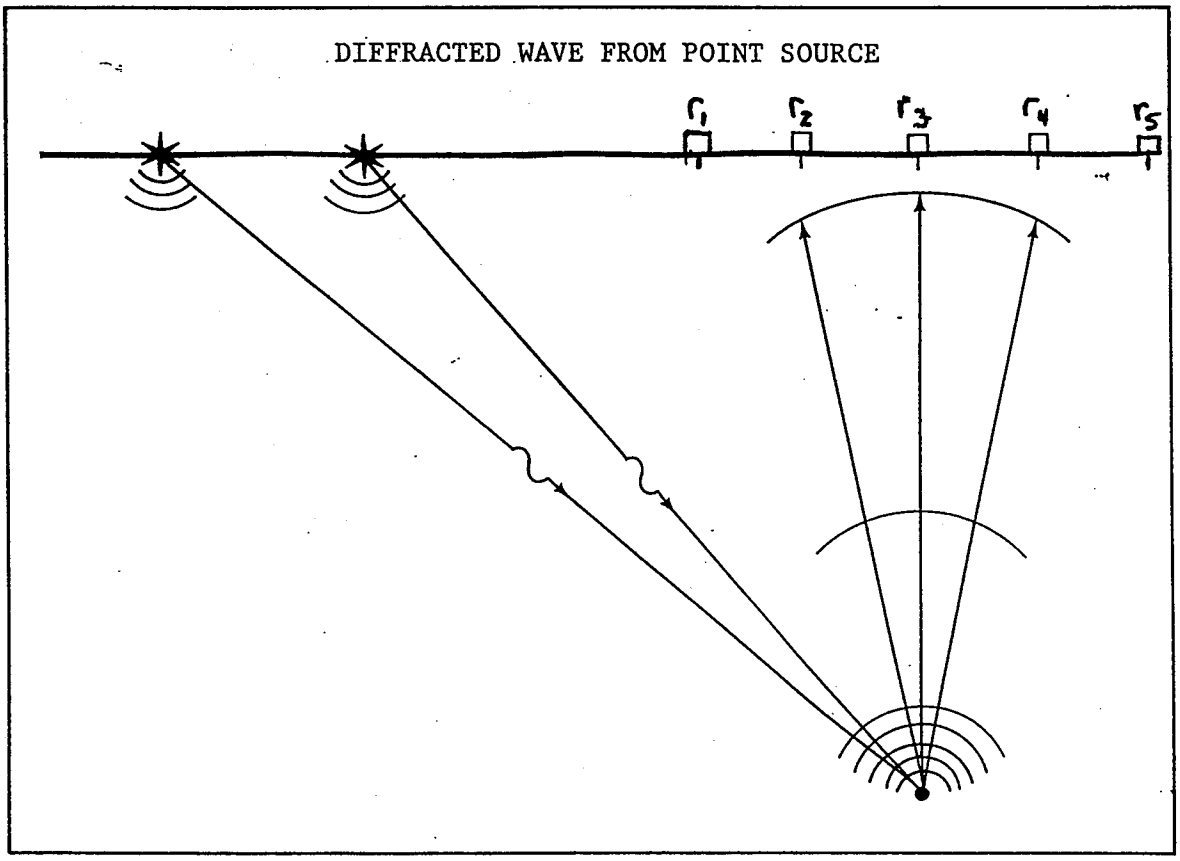

Figure 4

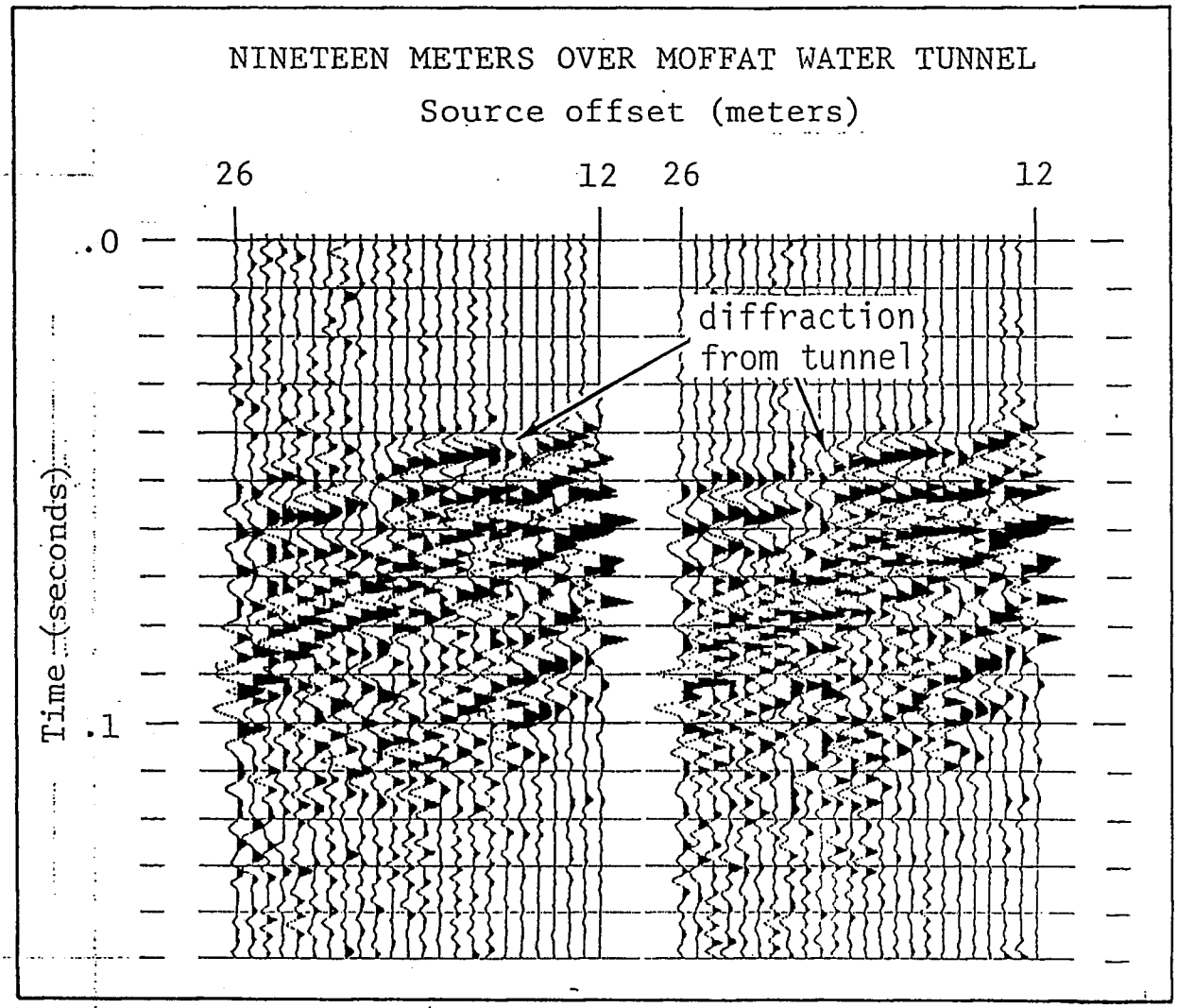
NINETEEN METERS OVER MOFFAT WATER TUNNEL
Source offset (meters)
26
12
26
12
.0
.1
Time (seconds)
diffraction
from tunnel

Figure 5

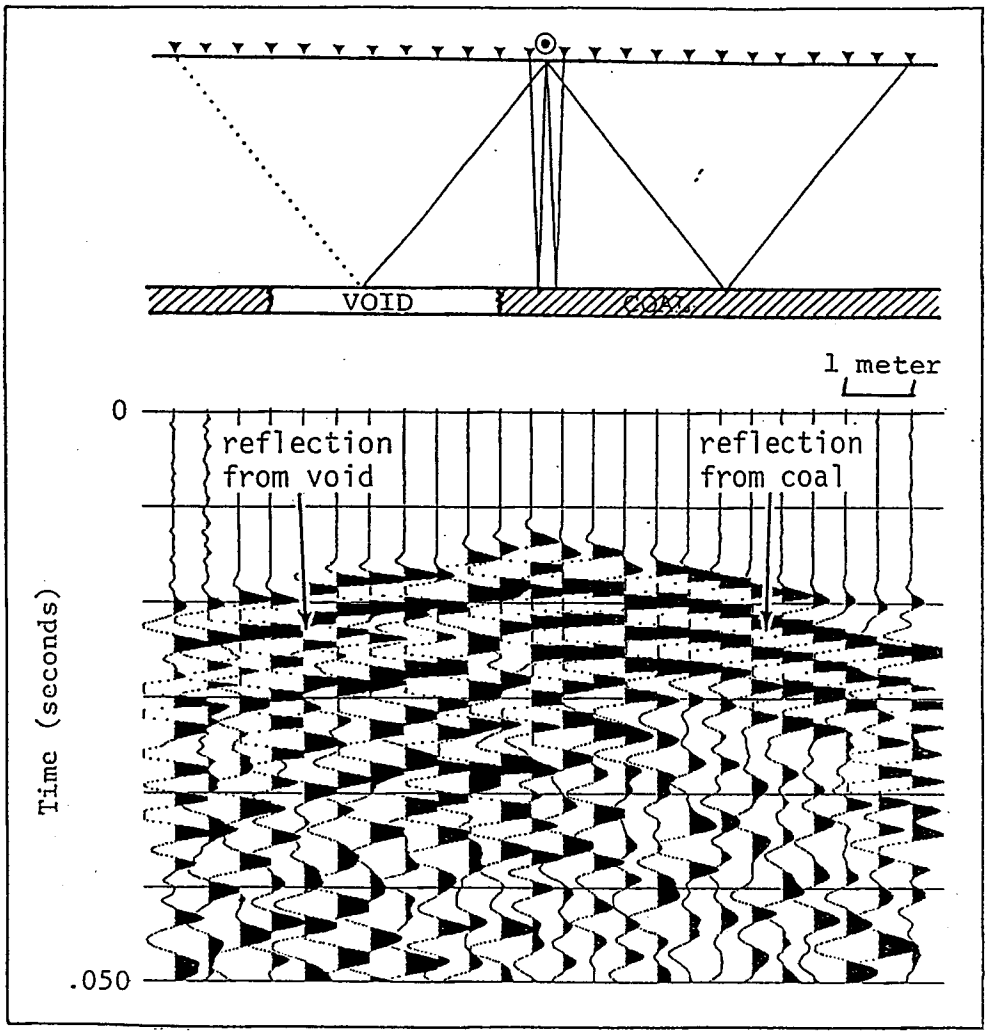
VOID
COAL
1 meter
0
reflection
from void
reflection
from coal
Time (seconds)
.050

Figure 6

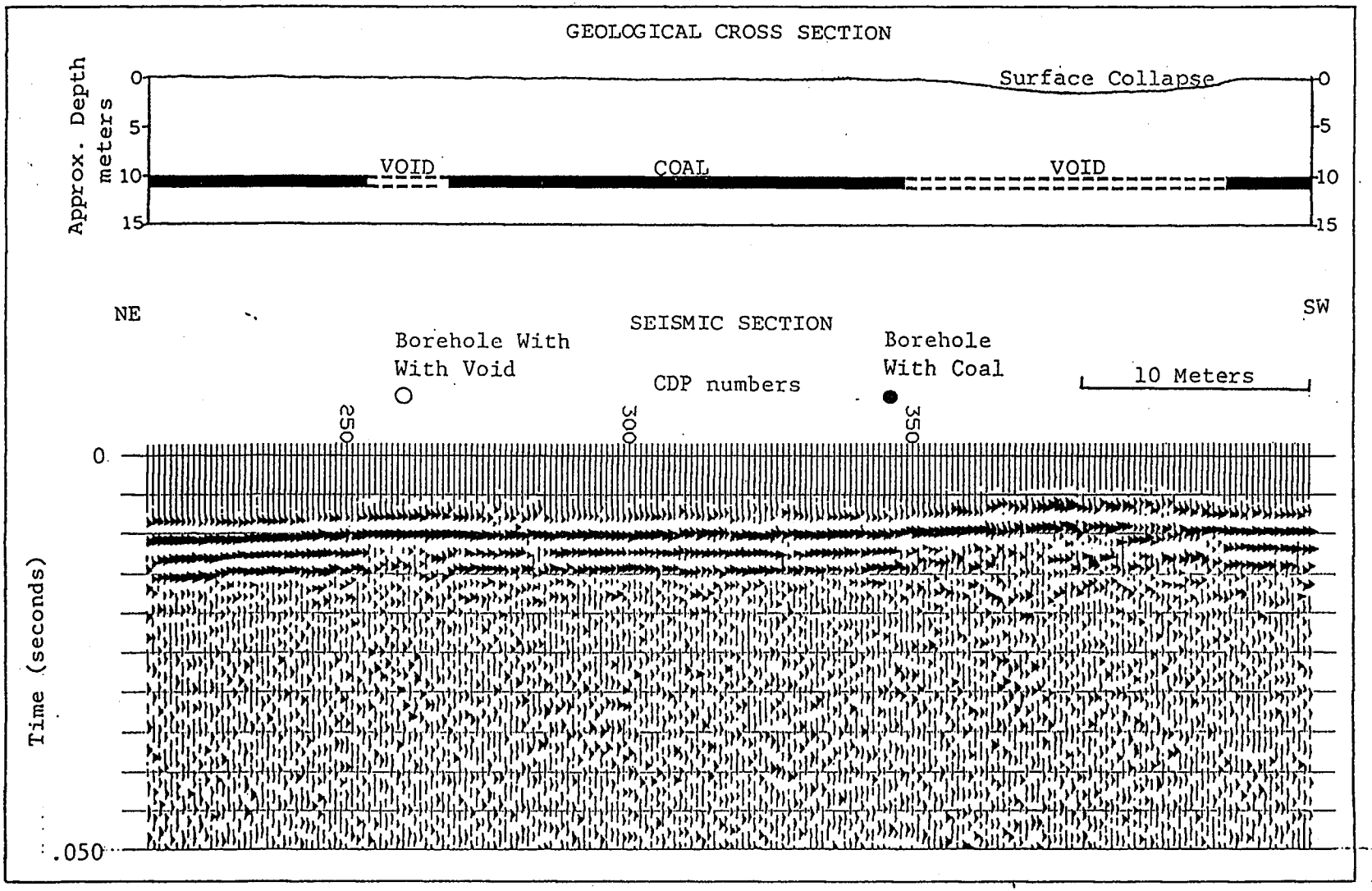
GEOLOGICAL CROSS SECTION
Approx. Depth meters
0
5
10
15
Surface Collapse
VOID
COAL
VOID
NE
SW
SEISMIC SECTION
Borehole With With Void
Borehole With Coal
CDP numbers
10 Meters
250
300
350
0
Time (seconds)
.050

Figure 7

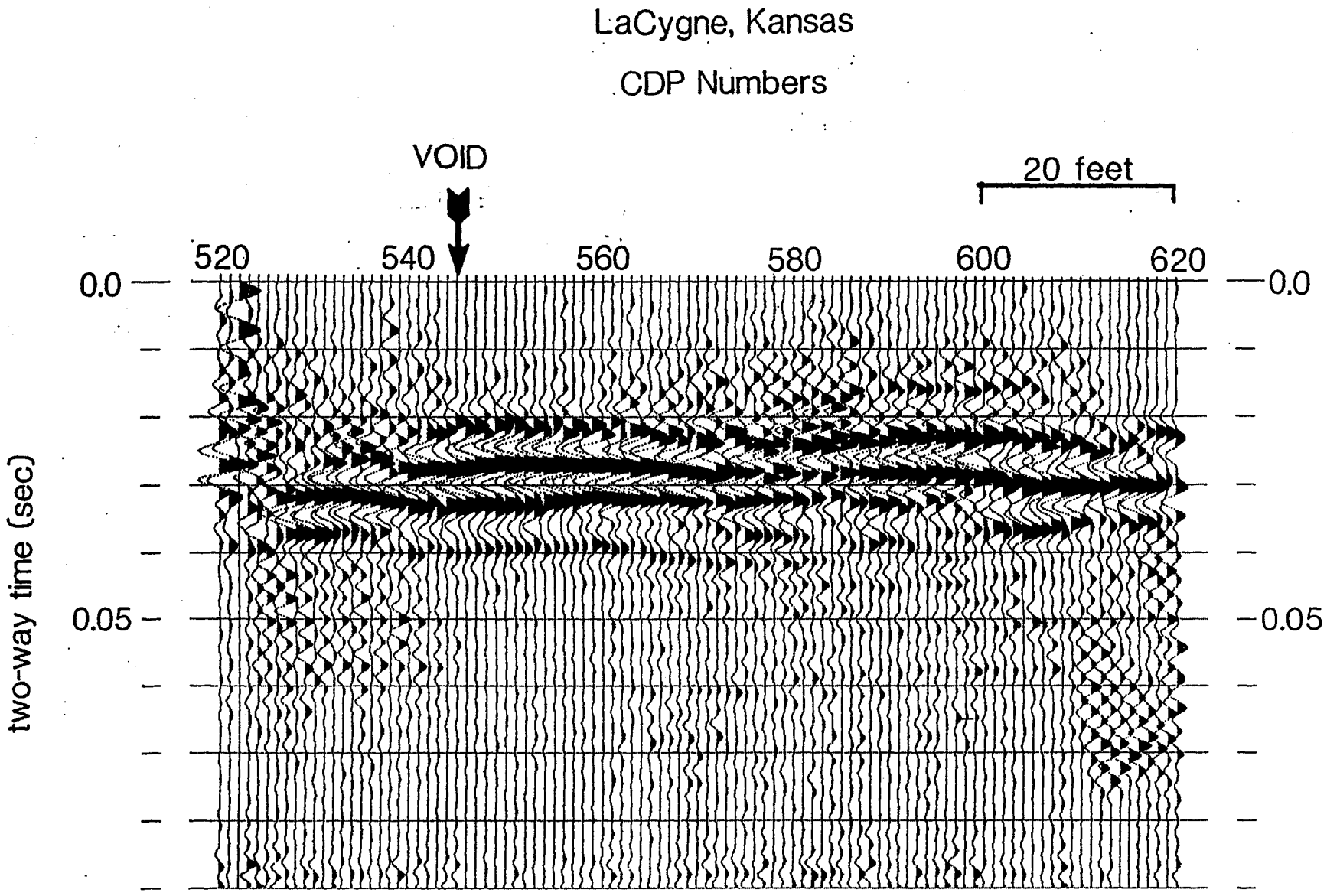
LaCygne, Kansas
CDP Numbers
VOID
20 feet
520
540
560
580
600
620
0.0
0.05
two-way time (sec)

Figure 9

Diffraction Enhancement

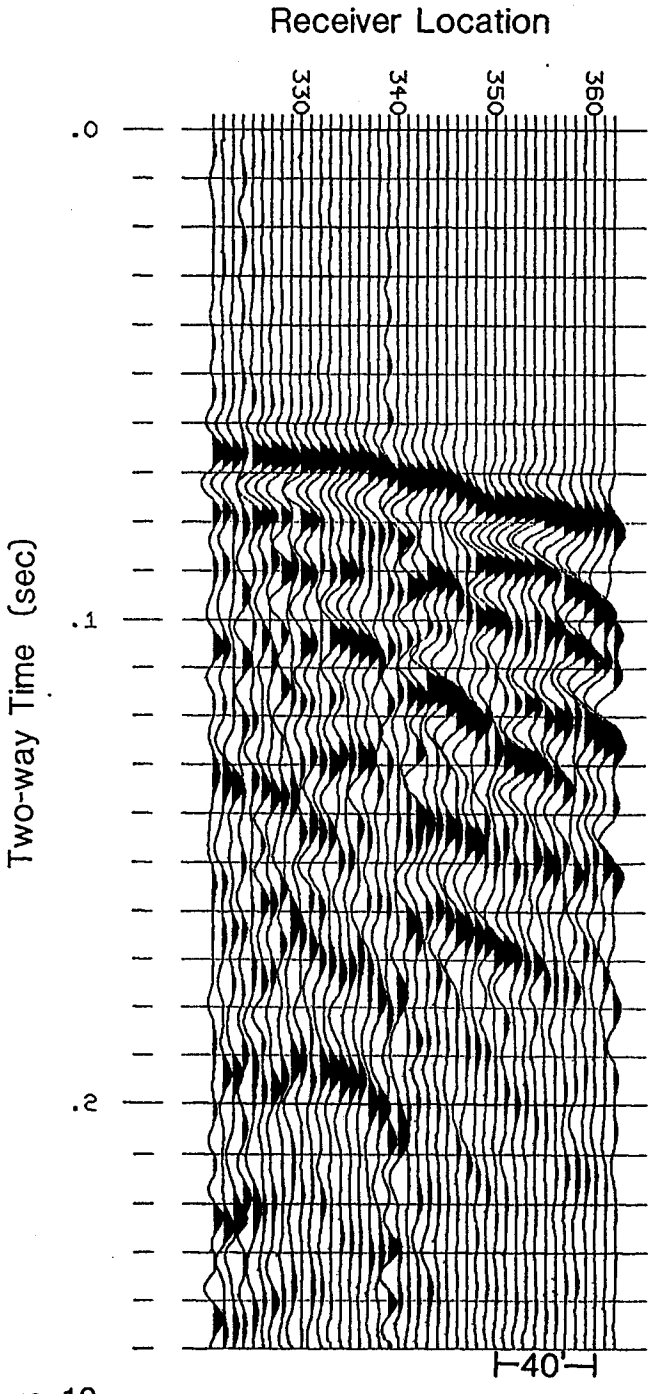

Figure 12.

Diffraction Enhancement

Moved-out

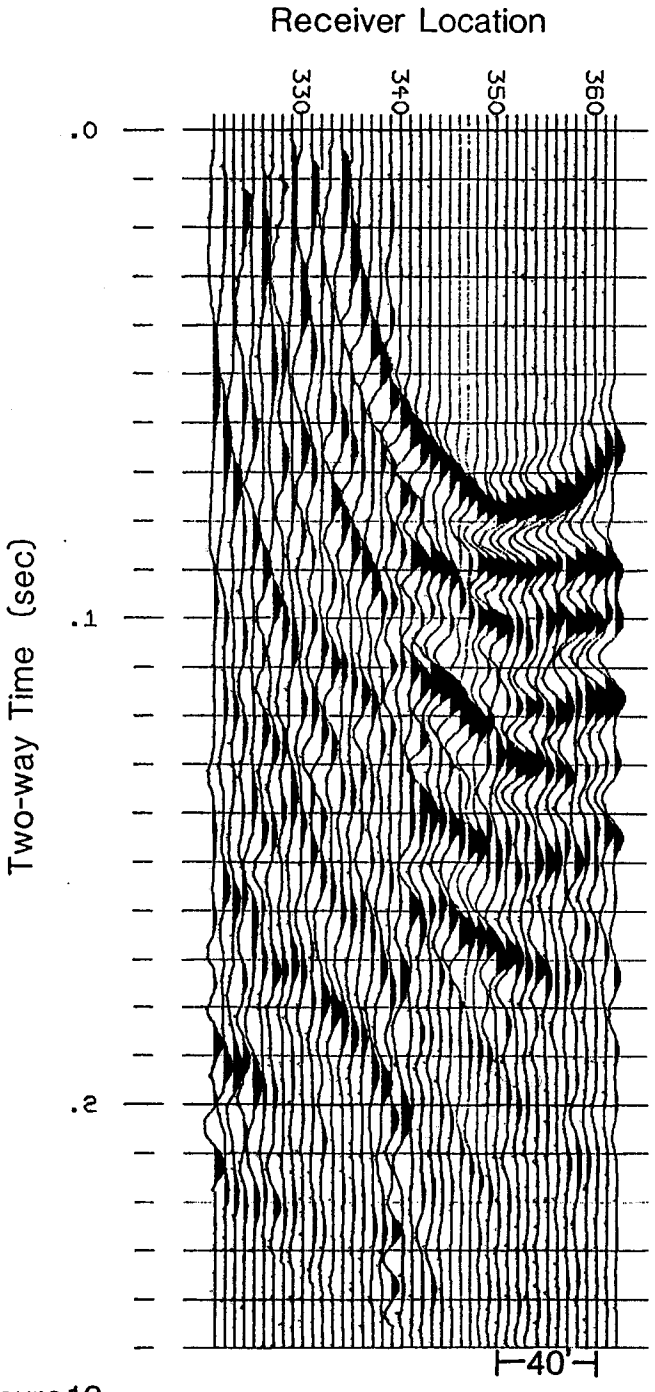

Figure 13.